

Research Article

Hypoxia macrophage-derived exosomal miR-26b-5p targeting PTEN promotes the development of keloids

Siya Dai^{1,†}, Mingyuan Xu^{1,†}, Qianqian Pang², Jiaqi Sun¹, Xiaohu Lin³, Xi Chu¹, Chunyi Guo¹ and Jinghong Xu^{1,*}

¹Department of Plastic Surgery, First Affiliated Hospital, School of Medicine, Zhejiang University, 79 Qingchun Road, Shangcheng District, Hangzhou, China, ²Department of Plastic Surgery, Ningbo Second Hospital, 41 Xibei Street, Ningbo, China and ³Department of Plastic and Reconstructive Surgery, Zhejiang Provincial People's Hospital, 158 Shangtang Road, Gongshu District, Hangzhou, China

*Correspondence. 1304017@zju.edu.cn

[†]Siya Dai and Mingyuan Xu contributed equally to this work.

Received 25 December 2022; Revised 11 May 2023; Accepted 21 June 2023

Abstract

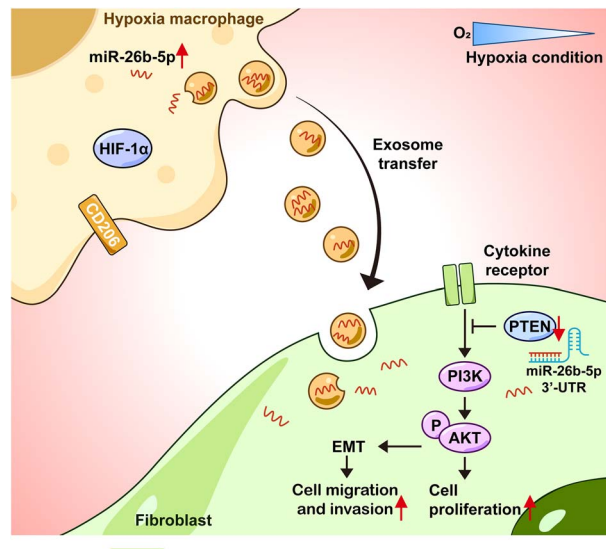
Background: Hypoxia is the typical characteristic of keloids. The development of keloids is closely related to the abnormal phenotypic transition of macrophages. However, the role of exosomal microRNAs (miRNAs) derived from hypoxic macrophages in keloids remains unclear. This study aimed to explore the role of hypoxic macrophage-derived exosomes (HMDE) in the occurrence and development of keloids and identify the critical miRNA.

Methods: The expression of CD206⁺ M2 macrophage in keloids and normal skin tissues was examined through immunofluorescence. The polarization of macrophages under a hypoxia environment was detected through flow cytometry. The internalization of macrophage-derived exosomes in human keloid fibroblasts (HKFs) was detected using a confocal microscope. miRNA sequencing was used to explore the differentially expressed miRNAs in exosomes derived from the normoxic and hypoxic macrophage. Subsequently, the dual-luciferase reporter assay verified that phosphatase and tension homolog (PTEN) was miR-26b-5p's target. The biological function of macrophage-derived exosomes, miR-26b-5p and PTEN were detected using the CCK-8, wound-healing and Transwell assays. Western blot assay was used to confirm the miR-26b-5p's underlying mechanisms and PTEN-PI3K/AKT pathway.

Results: We demonstrated that M2-type macrophages were enriched in keloids and that hypoxia treatment could polarize macrophages toward M2-type. Compared with normoxic macrophage-derived exosomes (NMDE), HMDE promote the proliferation, migration and invasion of HKFs. A total of 38 differential miRNAs (18 upregulated and 20 downregulated) were found between the NMDE and HMDE. miR-26b-5p was enriched in HMDE, which could be transmitted to HKFs. According to the results of the functional assay, exosomal miR-26b-5p produced by macrophages facilitated HKFs' migration, invasion and proliferation via the PTEN-PI3K/AKT pathway.

Conclusions: The highly expressed miR-26b-5p in HMDE promotes the development of keloids via the PTEN-PI3K/AKT pathway.

Graphical Abstract



Key words: Hypoxia, Keloid, Macrophage, Exosome, miR-26b-5p, Phosphatase and tension homolog

Highlights

- The hypoxic environment of keloids promotes the polarization of macrophages to the M2 type and the release of macrophage-derived exosomes.
- Hypoxic macrophage-derived exosomes facilitate the proliferation, migration, and invasive abilities of human keloid fibroblasts.
- Upregulated miR-26b-5p in hypoxic macrophage-derived exosomes promotes keloids development via the PTEN-PI3K/AKT pathway.

Background

Keloid is a common fibroproliferative skin disease characterized by aggressive fibroblast proliferation and excessive extracellular matrix (ECM) accumulation [1,2]. Although keloids are generally considered benign fibroproliferation, they often exhibit malignant properties such as persistent and aggressive growth [3]. Surgery combined with local irradiation, steroid injection and compression therapy are the main methods used to treat keloids [4]. However, keloids are highly prone to recurrence regardless of drug or surgical treatment, and there is currently no satisfactory treatment.

Under different microenvironments, macrophages can polarize into either pro-inflammatory M1- or anti-inflammatory M2-type and M2-type macrophages are crucial for the inducing skin fibrosis during wound healing [5]. Macrophages undergo conversion from M1 to M2 type during wound healing [6,7]. Pathological wound healing may result from abnormal switching of macrophage subtypes [8]. The occurrence and development of keloids are significantly

influenced by macrophages [9,10]. Keloids have an increased proportion of M2-type macrophages compared to normal skin [11]. Furthermore, the marginal region of keloids exhibits high M2-type macrophage expression, which may be related to the invasive properties of keloids [12].

Hypoxia-inducible factor-1 (HIF-1) is assumed to be the key transcriptional regulator that regulates the biological behavior of cells under a hypoxic environment [13]. Several studies have documented the elevated expression of HIF-1 α in keloids, indicating that keloids contain a hypoxic environment [14–17], which may be associated with their extensive microvascular obstruction, malformation, fibroblast proliferation and increased collagen expression [18,19]. Hypoxia may be crucial in the occurrence and development of keloids through multiple pathways [17–19]. By activating the TGF- β /Smad3 signal pathway, hypoxia encourages fibroblasts to transform into myofibroblasts [20]. Hypoxia could alter the glucose metabolism and cell function of keloid fibroblasts [15]. Our earlier research also demonstrated that HIF-1 α

promotes keloid formation by activating TGF- β /Smad and TLR4/MyD88/NF- κ B pathways in keloid fibroblasts [17]. Furthermore, clinical studies have suggested that hyperbaric oxygen therapy can lower the recurrence rate of keloid after surgery and radiotherapy [21]. These investigations collectively demonstrated that hypoxia is closely associated with keloids. However, it has not yet been reported whether the hypoxic environment of keloid affects macrophage phenotype.

Exosomes are 30–150 nm diameter lipid bilayer membrane vesicles that mediate intercellular communication [22]. Exosomal miRNAs, the main contents carried by exosomes, can be transported to recipient cells alongside exosomes, which are crucial for the post-transcriptional regulation of genes [23–25]. The association between dysregulated miRNA expression and keloids has received extensive attention. Numerous keloid miRNAs have been identified to play a role in regulating cell behavior, such as abnormal proliferation [26], autophagy [27], apoptosis [28], cell cycle [26], migration [27] and collagen production [29]. However, no study has investigated how miR-26b-5p contributes to the development of keloids yet.

In this study, we confirmed that the hypoxic environment of keloids promotes macrophage polarization to the M2 type. We proved that miR-26b-5p was shuttled directly from hypoxic macrophages to HKFs via exosomes, where it targeted and downregulated PTEN expression, thereby promoting HKFs' proliferation, migration and invasion.

Methods

Patient samples

In accordance with the Clinical Research Ethics Committee's permission, keloid and normal skin tissues were obtained from 64 patients at the Department of Plastic Surgery of First Affiliated Hospital, School of Medicine, Zhejiang University. All samples were selected from patients without any previous treatments and were confirmed to be keloids or normal skin by pathological examination, and they had never received treatment. Table S1 presents the clinical and demographic information of patients. Before surgery, each patient signed an informed consent, and all experiments were carried out after approval (no. 2014058; 27 February 2014).

Cell lines and cell culture

HKFs were derived from patients who underwent keloid excision surgery. After removing the epidermis, keloids were minced into pieces and then digested with trypsin (GIBCO BRL, USA) and 2.0 mg/ml type I collagenase (Solarbio, China). They were then cultured in DMEM (Servicebio, China) containing 10% FBS (GIBCO BRL, USA), 100 U/ml penicillin and 100 μ g/ml streptomycin for 5 days. HKFs were cultured in an incubator with 5% CO₂ at 37°C, used from passages three to nine.

Human leukemia monocyte THP-1 cell line was obtained from the Shanghai Institute of Cell Biology at the China

Academy of Sciences. THP-1 cells were cultured in 1640 (Servicebio, China) containing 10% FBS, 100 U/ml penicillin and 100 μ g/ml streptomycin, and passaged for <3 months after resuscitation. To induce THP-1 cells into macrophages, 100 ng/ml phorbol 12-myristate 13-acetate (PMA, Sigma-Aldrich, USA) was added for 24 h. Macrophages were labeled with CD68 antibodies and identified using LSRII flow cytometer (BD Biosciences, USA).

For hypoxic conditions, macrophages were cultured in a modular incubator chamber with 94% N₂, 5% CO₂ and 1% O₂ concentration at 37°C.

Immunofluorescence staining

After being fixed in 4% paraformaldehyde and embedded in paraffin, keloids and skin tissues were sectioned to a thickness of 4 μ m. Sections were exposed to the primary antibodies CD68 (1:100; EBioscience, USA, 14-0688-82) and CD206 (1:100; Cell Signaling Technology, USA, 91992) for an overnight incubation at 4°C following deparaffinization, rehydration and antigen retrieval. After that, sections were incubated with secondary antibody for 1 h at room temperature away from light. A fluorescence microscope (Leica DMI6000B, Germany) was used to capture the images.

Immunohistochemistry and scoring

Tissue sections were deparaffinized, rehydrated and then blocked with 3% BSA before being incubated with antibodies against PTEN (1:100; Santa Cruz Biotechnology, USA, sc-7974) and HIF-1 α (1:200; Proteintech Group, USA, 20960-1-AP). Six fields (\times 200) were randomly selected for each section. Two qualified pathologists independently scored the immunohistochemistry (IHC) images. On the basis of the percentage of cells, the staining intensity was graded from 0 to 4: no positive cells were classified as 0, <25% as 1, 25–50% as 2, 50–75% as 3 and >75% as 4.

Exosomes isolation, characterization and quantification

Exosomes were collected from the macrophage culture medium (CM) through ultracentrifugation. To remove cells and debris, the cell culture medium was centrifuged at 300 g for 5 min and 3000 g for 30 min. The medium was then added to ultrafiltration tubes (100 kDa, Merck Millipore, USA) and centrifuged at 4000 g for 5 min. The exosomes were collected by centrifugation at 150,000 g for 2 h. After resuspension in PBS the exosomes were purified again through ultracentrifugation.

The size and shape of exosomes were verified through transmission electron microscopy (TEM). Exosomes were diluted 100 times using PBS, dropped into carbon-coated copper grids and stained with 2% glutaraldehyde. After the copper grids had dried, the Tecnai G2 Spirit electron microscope (Thermo Fisher Scientific, USA) was used to capture stained images.

The sizes and concentrations of exosomes were detected through nanoparticle tracking analysis (NTA) and calculated using ZetaView (Particle Metrix, Germany). Exosomes were

diluted 500 times by PBS and fully resuspended before being injected into the sample pool. According to the measured concentrations, the exosome solutions of different samples were adjusted to the same concentration by PBS.

Exosome labeling and tracking

Following the manufacturer's instructions, exosomes were labeled using a PKH67 green fluorescent cell linker kit (Sigma-Aldrich, USA) and cultured with HKFs for 12 h. A Leica TCS SP5 II laser scanning confocal microscope was used to record the ingestion of exosomes by HKFs.

miRNA sequencing

Following the manufacturer's instructions, sequencing libraries were created using QIAseq miRNA Library Kit (Qiagen, Germany) and index codes were added to assign sequences to specific samples. To investigate the quantification of miRNA expressions, reverse transcription primers with unique molecular indices were introduced during cDNA synthesis and PCR amplification. Using Agilent Bioanalyzer 2100 and qPCR, library quality was evaluated. The indexed sample clustering was carried out on the acBot Cluster Generation System utilizing TruSeq PE Cluster Kitv3-cBot-HS (Illumina, USA). The library preparations were sequenced on an Illumina NovaSeq 6000 platform and paired-end reads were produced at EchoBiotech Co. Ltd (China).

Quantitative real-time PCR analysis

Total RNA from cells and tissues was extracted using the TRIzol reagent (Invitrogen, USA), and reverse transcription of RNA into cDNA was performed using the PrimeScript RT kit (TaKaRa, Japan).

The expression of miRNA and mRNA was measured using quantitative real-time PCR (qRT-PCR) with SYBR Green Kit (TaKaRa, Japan), which was then analyzed using the $2^{-\Delta\Delta C_t}$ method and normalized to U6 snRNA and GAPDH, respectively. Table 1 shows the primer sequences.

Transfection

The miRNA mimics, miRNA inhibitor, siRNAs against PTEN and the negative control were all synthesized by RiboBio Co., Ltd (China) and verified using qRT-PCR.

Following the manufacturer's instructions, HKFs were transfected with 50 nM RNA or negative control using the jet-PRIME transfection reagent (Polyplus Transfection, France). Table 2 shows the primer sequences.

Western blot analysis

Cell and tissue protein was extracted using RIPA buffer (Beyotime, China). Proteins (20-30 mg) were separated by 10% sodium dodecyl-sulfate polyacrylamide gel electrophoresis gel before being transferred to polyvinylidene difluoride membranes (Merck Millipore, USA). After being blocked in 5% milk for 1 h, the membranes were then probed

Table 1. The primer sequences

Primer	Sequence (5'-3')
miR-26b-5p	CGAGCGCTTCAAGTAATTCAGGATAGG
miR-210-3p	AAGTTGTCTGTGCGTGTGAC
miR-31-5p	AACACGCAGGCAAGATGCTG
miR-155-5p	CGCCTTAATGCTAATCGTGATAGGGGT
U6	Forward:TGGAACGCTTCACGAATTTGCCG Reverse:GGAACGATACAGAGAAGATTAGC
GAPDH	Forward:GGAGCGAGATCCCTCCAAAAT Reverse:GGCTGTTGTCATACTTCTCATGG
PTEN	Forward:CTCAGCCGTTACCTGTGTGT Reverse:AGGTTTCCTCTGGTCCTGGT
HIF-1 α	Forward:TGATTGCATCTCCATCTCCTACC Reverse:GACTCAAAGCGACAGATAACACG
CD206	Forward:TCCTAGTCAGTGGTGGCCGTATG Reverse:CGATGGTGTGGATACTTGTGAGGTC
DC-SIGN	Forward:TGCTGAGGAGCAGAACTTCC Reverse:GTTGGGCTCTCTCTGTTC
TGF- β	Forward:GGATCTCTGTGTATTGGGC Reverse:CAACAGTGCCCAAGGTGCT

Forward forward primer, Reverse reverse primer, PTEN phosphatase and tension homolog, HIF-1 α hypoxia-inducible factor-1 α , TGF- β transforming growth factor- β

Table 2. The primer sequences

RNA	Sense (5'-3')
miRNA-26b-5p mimics	UUCAAGUAAUUCAGGAUAGGU CUAUCCUGAAUUACUUGAAUU
NC mimics	UUGUACUACACAAAAGUACUG GUACUUUUGUGUAGUACAAUU
miR-26b-5p inhibitor	ACCUAUCCUGAAUUACUUGAA
NC inhibitor	CAGUACUUUUGUGUAGUACAA
si-PTEN	GGAGGAUUUUCGUCUUCUTT AGAAGACGAAUUAUCCUCCTT

PTEN phosphatase and tension homolog

at 4°C overnight with antibodies against PTEN (1:500; Santa Cruz Biotechnology, USA, sc-7974), AKT (1:1000; Proteintech Group, USA, 10176-2-AP), p-AKT (1:1000; Proteintech Group, USA, 66444-1-Ig), HIF-1 α (1:1000; Proteintech Group, USA, 20960-1-AP), MMP9 (1:1000; Proteintech Group, USA, 10375-2-AP), Collagen Type I (1:1000; Proteintech Group, USA, 14695-1-AP), E-cadherin (1:1000; Proteintech Group, USA, 20874-1-AP), Smooth Muscle Actin (1:1000; Proteintech Group, USA, 14395-1-AP), CD63 (1:1000; Proteintech Group, USA, 25682-1-AP), CD81 (1:1000; Proteintech Group, USA, 66866-1-Ig), HSP70 (1:1000; Abcam, USA, ab5439), β -Tubulin (1:5000; Cell Signaling Technology, USA, 2146) and GAPDH (1:5000; Abcam, USA, ab8245). The membranes were washed by TBS with Tween, then incubated with horseradish peroxidase-conjugated secondary antibodies for 1 h. After that, the membranes were immersed in ECL (Abbkine, China) and visualized using a chemiluminescence instrument.

Luciferase reporter assay

By using FuGENE 6 Transfection Reagent (Promega, USA), HKFs were transiently co-transfected with wild-type or mutant 3' untranslated region (UTR) of PTEN and miR-26b-5p mimics or mimics-NC. The firefly and renilla luciferase activities were measured consecutively using the Dual-Luciferase Reporter assay system (Promega, USA). Firefly luciferase's relative luminescence intensity was normalized to that of renilla luciferase.

Flow cytometric analysis

Macrophages were fixed in fixation buffer (Thermo Fisher Scientific, USA) for 20 min and then washed with staining perm wash buffer (Thermo Fisher Scientific, USA). Fc blocker (BioLegend, USA, 422301) was used to block the Fc receptor. The following antibodies were used: PerCP/Cyanine5.5 anti-human CD68 (BioLegend, USA, 333813) and FITC anti-human CD206 (BioLegend, USA, 321103). An LSRII flow cytometer (BD Biosciences, USA) was used to acquire and analyze the expression of macrophage proteins.

Cell proliferation assay

Cells were plated into 96-well plates (3×10^3 cells/well), and 200 μ l of CCK-8 solution was added to each well after 24, 48, 72 and 96 h of incubation. The OD value was determined at 450 nm using a microtiter plate reader after 2 h of incubation.

Transwell assay

For invasion and migration assays, $\sim 300 \mu$ l of HKFs were resuspended in serum-free DMEM and deposited onto an 8-mm-pore-size Transwell chamber (BD Falcon, USA) with and without Matrigel (Corning Incorporated, USA). The lower chamber was filled with 800 μ l of the serum-containing medium. Cells in the upper part were removed using a cotton swab after 48 h of incubation. Cells adhering to the lower membrane were fixed with the fixative solution, stained with staining solution (Wright-Giemsa Stain Kit, Nanjing Jiancheng Institute of Bioengineering, China) and then recorded using a phase contrast microscope (Olympus, Japan). After being rinsed with 33% acetic acid, the crystal violet-stained cells were measured for absorbance at 570 nm.

Scratch wound-healing assay

The cells were first seeded into culture inserts (Ibidi, Germany). After the cells had adhered to the bottom, the culture inserts were removed. The wound area was recorded with a phase contrast microscope and measured with ImageJ at 0 and 24 h after the culture inserts were removed.

Statistical analysis

The results from at least three independent replicates were presented as mean \pm SD. SPSS and GraphPad Prism v.9.0 were used to conduct statistical analyses. The Student's *t*-test

was used to analyze independent and normally distributed paired data. The one-way ANOVA test was used to analyze independent, normally distributed and homogeneous variance data with one independent variable, whereas the two-way ANOVA test was used with two independent variables. The Bonferroni method was used as a *post hoc* test following ANOVA. The Mann-Whitney test was used to analyze independent but not normally distributed data. A statistically significant difference was $p < 0.05$.

Results

Hypoxia triggers macrophages to polarize to M2 type

To explore the internal microenvironment of keloids, we collected 35 keloid tissues and 29 normal skin tissues excised by clinical surgery. The detailed source information of tissues is listed in Table S1 (in the online supplementary material). In keloid, histological staining revealed many thick and dense collagen fibers with an irregular arrangement, whereas collagen fibers in normal skin were sparse and regularly arranged (Figure S1a, see online supplementary material for a color version of this figure). As evident in Figures 1a–d, HIF-1 α expression in keloids was significantly higher than in normal skin tissues, indicating that keloids have a hypoxic environment.

We characterized the number and distribution of M2 macrophages in keloids and normal skin tissues through immunofluorescence staining. The results revealed that keloid tissue contained significantly more CD206⁺ M2 macrophages than normal skin tissue (Figure 1e). Keloids are thought to be abundant in M2-type macrophages.

By using PMA, THP-1 monocytes were induced into macrophages. The macrophages were then either cultured in a normoxic or a hypoxic (1% O₂) incubator for 48 h. We first detected HIF-1 α protein expression in macrophages to determine whether the experimental conditions successfully induced hypoxic stress. Figure S1b demonstrates that CD68 expression exhibited in both normoxic and hypoxic macrophages, but HIF-1 α expression only exhibited in hypoxic macrophages. We determined whether a hypoxic environment could induce macrophage polarization through flow cytometry for the M2 marker CD206 in macrophages. Figure 1f–g shows that the proportion of CD206⁺ cells in hypoxic macrophages was 23.6%, which is significantly higher than that in normoxic macrophages (8.56%). M2 typical markers such as CD206, DC-SIGN and TGF- β were also highly expressed in hypoxic macrophages (Figure 1h). These data indicate that hypoxic macrophages had an M2-skewed phenotype.

Hypoxic macrophage-derived exosomes (HMDE) enhance HKFs' proliferation, migration and invasion

HKFs were isolated and cultured from keloid tissues and two of them, HKF1 and HKF2, were selected for subsequent experimental research. The impact of hypoxic macrophage CM on HKFs' proliferation ability was investigated using the CCK-8 assay. In the CCK-8 assay (Figure S1e–f), HKFs

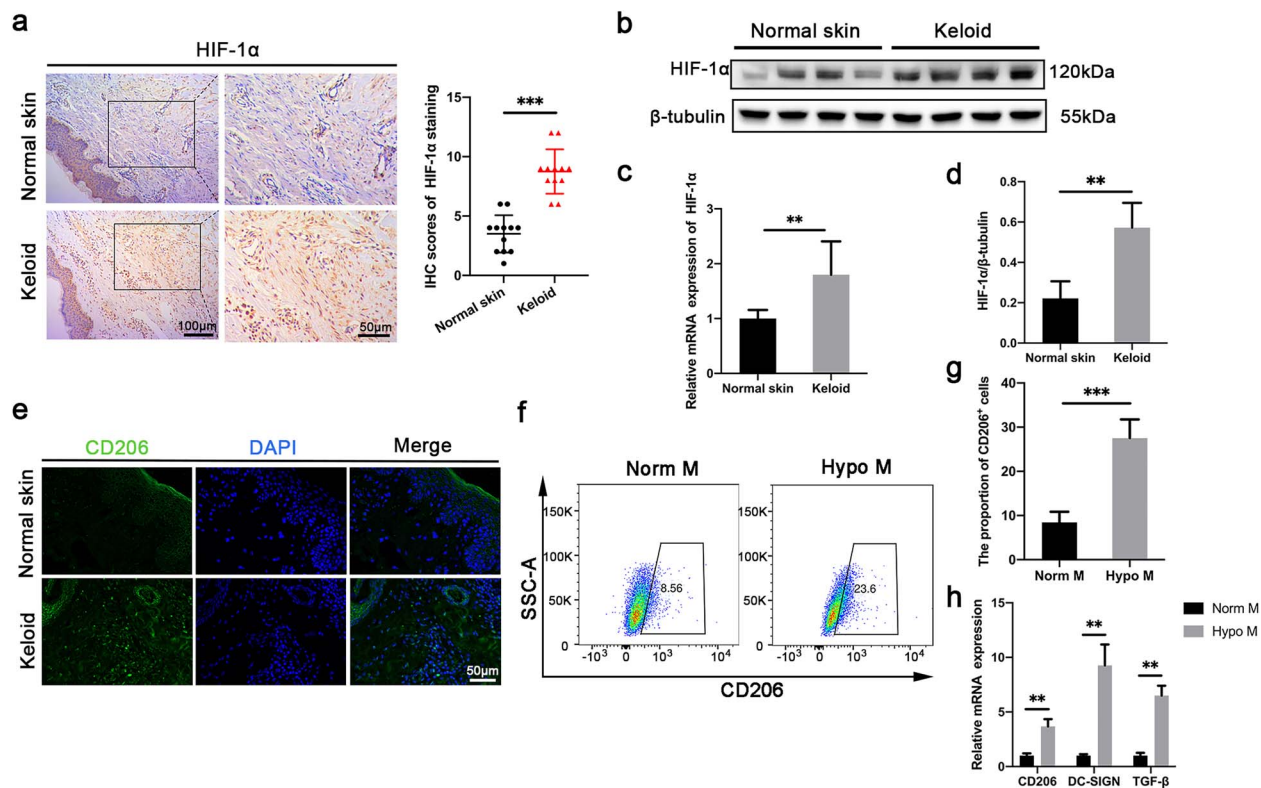


Figure 1. Hypoxia trigger macrophages to polarize to M2 type. (a) HIF-1 α expression tested using IHC analysis. (b) Western blot. (c) qRT-PCR. (d) The relative expression of HIF-1 α . (e) The number and distribution of M2 macrophages in keloids and normal skin tissues by immunofluorescence staining. (f) Validation of M2 macrophages using the M2 macrophage marker CD206 by flow cytometry. (g) Average counts from independent tests conducted three times. (h) qRT-PCR analyses of CD206, DC-SIGN and TGF- β mRNA levels in normoxic or hypoxic macrophages. ** $p < 0.01$, *** $p < 0.001$. Norm M normoxic macrophage, Hypo M hypoxic macrophage, HIF-1 α hypoxia inducible factor-1 α , TGF- β transforming growth factor- β

treated with hypoxic macrophage CM proliferated more than that treated with normoxic macrophage CM or FBS-free medium. The effects of hypoxic macrophage CM on HKFs' migration and invasion ability were investigated using the scratch and Transwell assays. In the scratch assay (Figure S1c), HKFs treated with hypoxic macrophage CM migrated more than normoxic macrophage CM or FBS-free medium. In the Transwell assay (Figure S1d), HKFs treated with hypoxic macrophage CM revealed an increase in cell migration and invasion compared to cells treated with normoxic macrophage CM or FBS-free medium.

The exosomes in the serum were then removed using ultracentrifugation, and the exosome-free serum was used to prepare a macrophage culture medium. For 48 h, equal amounts of macrophage were exposed to either normoxia or hypoxia, and the resulting CM was collected. We extracted exosomes from the CM through ultracentrifugation and resuspended the isolated exosomes in PBS. The purified exosomes from normoxic or hypoxic macrophages were examined using TEM, which revealed the presence of exosomes with diameters ranging from 120 to 150 nm and a double-layer cup-shaped morphology (Figure 2a). Exosomes were also verified using western blot. Figure 2b demonstrates that exosomal markers CD63 and CD81 were expressed in exosomes but not in cells, whereas GAPDH was expressed

in cells but not in exosomes. Membrane protein HSP70 was expressed both in exosomes and cells.

The role of hypoxia on macrophage exosome release was evaluated using NTA. The results demonstrated that exosome particles from normoxic and hypoxic macrophages had a similar peak at around 100 nm (Figure 2c–d). However, as shown in Figure 2e, the concentration of HMDE ($(25.0 \pm 7.0) \times 10^9$ particles/ml) was significantly higher than that of NMDE ($(9.4 \pm 3.0) \times 10^9$ particles/ml) particles/ml, suggesting that hypoxic macrophages secreted a greater number of exosomes than normoxic macrophages. The exosomes were adjusted to the same concentration by PBS for subsequent experiments based on the measured concentration.

We also detected whether HKFs could internalize macrophage exosomes. After 12 hours of incubation with either PKH67-labeled exosomes or PBS, confocal microscopy was used to monitor the internalization of exosomes in HKFs. We discovered that HKFs could take up both NMDE and HMDE and that the exosomes were mainly enriched in the cytoplasm (Figure 2f). To rule out the possibility of nonspecific binding, a tube of PBS was included during the PKH67 staining procedure. No fluorescence was observed in HKFs incubated with PKH67 labeled PBS, confirming the specificity of exosome absorption by HKFs.

Exosomes, once secreted, deliver biological information to nearby or distant cells via internalization. HKFs were

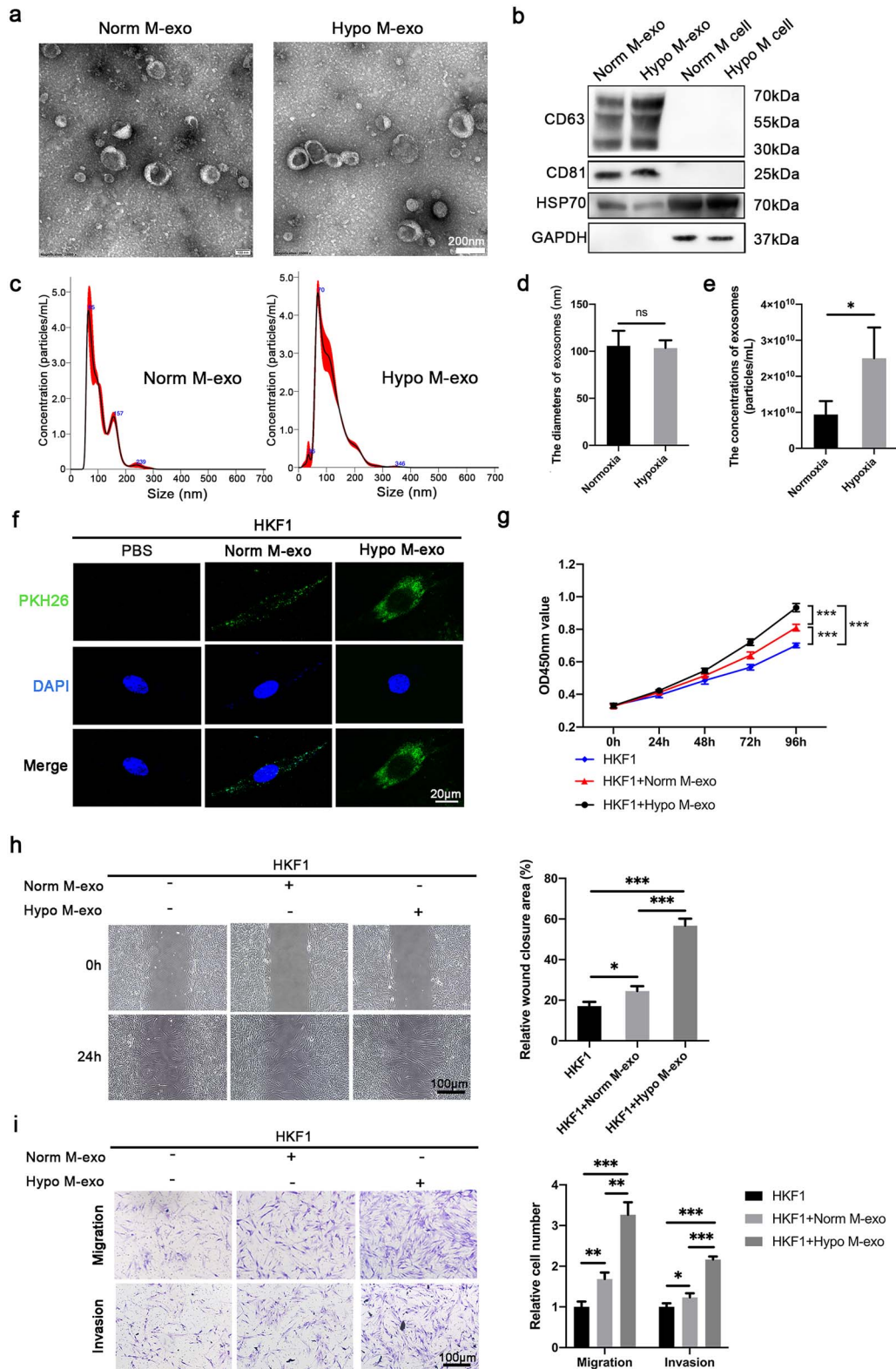


Figure 2. HMDE enhance HKF proliferation, migration and invasion. **(a)** Representative electron micrograph of macrophages-derived exosomes representing the typical morphology and size (120–150 nm). Scale bar: 200 nm. **(b)** Western blot analysis demonstrates the CD63, CD81, HSP70 and GAPDH expression in the exosomes (exo) and macrophages. **(c)** The concentration and diameter of exosomes derived from normoxic (Norm M-exo) or hypoxic (Hypo M-exo) macrophages. The diameter **(d)** and concentration **(e)** of exosomes. **(f)** Representative confocal microscopy images illustrating how HKFs internalize PKH67-labeled exosomes (green) derived from normoxic or hypoxic macrophages by HKFs. Scale bar: 20 μm . **(g)** CCK-8 assay represents the cell proliferation ability. **(h)** Wound-healing assay. Scale bar: 100 μm . **(i)** Cell migration and invasion assays using Transwell or Matrigel-coated Transwell. Scale bar: 100 μm . ns, no significance, * $p < 0.05$, ** $p < 0.01$, *** $p < 0.001$. HKF human keloid fibroblast, Norm M-exo normoxic macrophage derived exosomes, Hypo M-exo hypoxic macrophage derived exosomes, HSP70 heat shock protein 70, CCK-8 cell counting kit-8

treated with PBS and exosomes derived from normoxic or hypoxic macrophages to determine how macrophage exosomes affect the phenotype of HKFs. HMDE significantly enhanced cell proliferation, migration and invasion compared to NMDE. As expected, compared with HKFs containing NMDE or PBS, HKFs containing HMDE in the medium demonstrated increased proliferation, migration and invasion ability (Figures 2g–i and S1g–i). These data suggest that HMDE can promote the proliferation, migration and invasion of HKFs. However, the molecular mechanism needs further exploration.

HMDE regulates HKFs' migration and invasion depending on miRNAs

To identify the mechanisms of HMDE promoting HKFs' proliferation, migration and invasion, an RNA sequencing screening was performed using RNA extracted from macrophage exosomes. We then compared the miRNA profiles of NMDE and HMDE. Figure 3a–b shows noncoding RNA sequence analysis and reveal 38 miRNAs with an altered expression between NMDE and HMDE. Among 38 miRNAs, 18 were upregulated and 20 were downregulated in HMDE compared with NMDE.

We selected miR-26b-5p, miR-31-5p, miR-155-5p and miR-210-3p as candidate miRNA based on the miRNA sequencing results and the previous reports indicating their relation to hypoxia as well as their possible biological functions. Their expression in keloids and normal skin tissues was confirmed by using qRT-PCR. The results revealed that keloids had higher expressions of miR-26b-5p, miR-31-5p, miR-155-5p and miR-210-3p than normal skin (Figure 3c). We further verified whether hypoxia treatment could increase the expression of these miRNAs in HKFs. The aforementioned miRNAs were expressed similarly in normoxic- and hypoxic-treated HKFs, without discernible differences (Figures 3d and S2a). To verify the expressions of miR-26b-5p, miR-31-5p, miR-155-5p and miR-210-3p in HMDE, we used the NMDE as controls. The results demonstrated that HMDE revealed higher expressions of miR-26b-5p, miR-31-5p, miR-155-5p and miR-210-3p than controls (Figures 3e and S2b). These findings reveal that hypoxia stimulation enriches miR-26b-5p, miR-31-5p, miR-155-5p and miR-210-3p in the exosomes secreted by macrophages, but not in HKFs, implying that miR-26b-5p, miR-31-5p, miR-155-5p and miR-210-3p are transferred from hypoxic macrophages to recipient HKFs. We then assumed that macrophage-derived exosomes could transfer specific miRNAs into HKFs, thereby altering the phenotype of HKFs. After 48 h of incubation of NMDE, HMDE or PBS separately, the expressions of miR-26b-5p, miR-31-5p, miR-155-5p and miR-210-3p in HKFs were verified by qRT-PCR. As expected, HKFs treated with HMDE had significantly higher expressions of miR-26b-5p, miR-31-5p, miR-155-5p and miR-210-3p than those treated with NMDE or PBS (Figure 3f). These findings are consistent with the aforementioned exosomal-miRNA expression, suggesting that miRNAs can be transferred from

exosomes into HKFs. The elevation of miR-26b-5p among these miRNAs was most pronounced in HMDE compared with NMDE. Combined with the miRNA sequencing results and the previously reported biological functions, we further explored how miR-26b-5p affected the phenotype of HKFs.

To investigate the role of miR-26b-5p in HKFs, we either overexpressed miR-26b-5p with mimics or inhibited miR-26b-5p with inhibitors. After 48 h, the miR-26b-5p expression of HKFs was detected using qRT-PCR to verify transfection efficiency. As determined using qRT-PCR, the overexpression by miR-26b-5p mimics resulted in an increase of miR-26b-5p in HKFs, whereas the inhibition of miR-26b-5p resulted in a decrease of miR-26b-5p in HKFs (Figure S2c–d). Figures 3g–i and S2e–g show that miR-26b-5p upregulation increased cell proliferation, migration and invasion in HKFs while miR-26b-5p downregulation reduced cell proliferation, migration and invasion.

We confirmed that HMDE could promote the expression of fibrotic proteins and activate the epithelial-mesenchymal transition (EMT) pathways in HKFs. We subsequently explored whether modulating intracellular miR-26b-5p can affect the expression of HKFs fibrosis and EMT-related proteins (Figure 3j). The results demonstrated that the transfection of miR-26b-5p mimics significantly increased the protein expressions of MMP9 and α -SMA in HKFs while considerably decreasing the protein expression of E-cadherin. These findings indicate that miR-26b-5p upregulation can promote fibrosis and EMT of HKFs.

Exosmic miR-26b-5p inactivates PI3K/AKT pathway through PTEN targeting

Public databases including miRMap, PicTar, TargetScan, Starbase and miRDB were used to predict the target genes of miR-26b-5p. We found that PTEN is a downstream target of miR-26b-5p verified by multiple databases (Figure 4a). We also performed the luciferase reporter assay in HKFs, where miR-26b-5p mimics were co-transfected with wild-type or mutant PTEN 3'-UTR-driven luciferase vectors. The results showed that wild-type PTEN 3' UTR but not mutant PTEN 3' UTR had their luciferase activity suppressed by overexpression of miR-26b-5p (Figure 4b). Therefore, PTEN was confirmed as a direct target gene of miR-26b-5p. We examined PTEN expression in keloids and normal skin tissues through qRT-PCR, western blot and IHC assays. The results revealed that keloid PTEN expression was significantly lower than normal skin tissue (Figure 4c–f).

To examine the effect of miR-26b-5p on PTEN expression, we transfected miR-26b-5p mimics or its inhibitor into HKFs and then measured the levels of PTEN and p-AKT. According to western blot analysis, upregulation of miR-26b-5p in HKFs led to a significant downregulation of PTEN and an upregulation of p-AKT (phosphorylated on Ser473) (Figure 4g). By contrast, miR-26b-5p downregulation could upregulate PTEN and downregulate p-AKT. The abundance of p-AKT was inversely correlated with the expression of PTEN in HKFs.

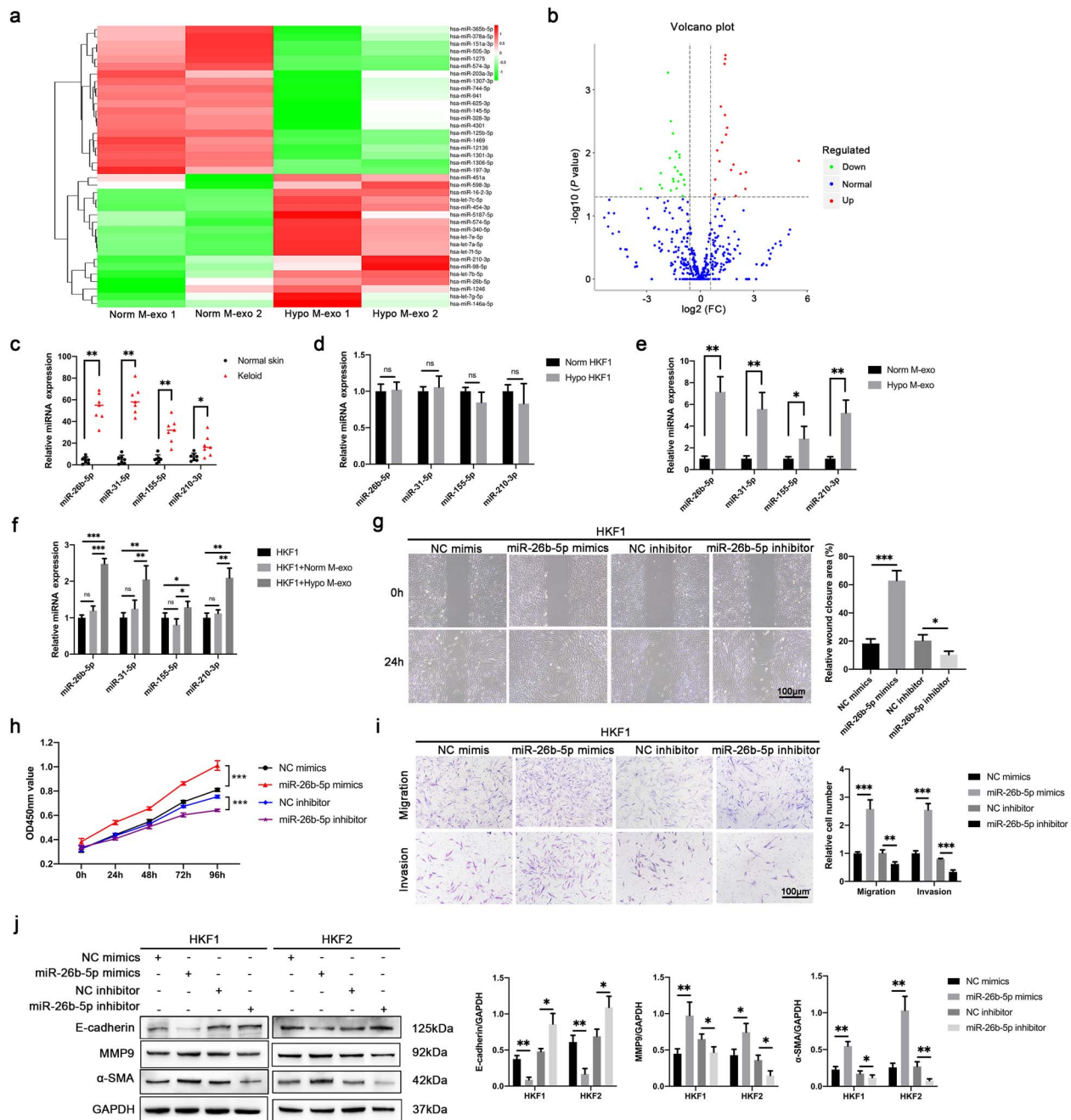


Figure 3. HMDE regulates HKFs' migration and invasion depending on miRNAs. The differential expression level of exosomal miRNAs between NMDE and HMDE. A heatmap (a) and volcano map (b). miR-26b-5p is one of the exosomal miRNAs with markedly higher abundance in Hypo M-exo compared to Norm M-exo. (c) miR-26b-5p, miR-31-5p, miR-155-5p and miR-210-3p expression in keloids and normal skin tissues. (d) miR-26b-5p, miR-31-5p, miR-155-5p and miR-210-3p expression in HKF1 after 24 h of normoxic or hypoxic treatment. (e,f) miR-26b-5p, miR-31-5p, miR-155-5p and miR-210-3p expression in exosomes and exosomes treated HKF1; HKF1 were transfected with miR-26b-5p mimics, miR-26b-5p inhibitor and their negative control, respectively. (g) CCK-8 assay represents the cell proliferation ability. (h) Wound-healing assay. Scale bar, 100 μ m. (i) Cell migration and invasion assays utilizing Transwell or Matrigel-coated Transwell. Scale bar: 100 μ m. (j) Western blot analysis measures the E-cadherin, MMP9 and α -SMA expression. ns not significant, * p < 0.05, ** p < 0.01, *** p < 0.001. Norm M-exo normoxic macrophage derived exosomes, Hypo M-exo hypoxic macrophage derived exosomes, miRNA microRNA, NC negative control, HKF human keloid fibroblas

HMDE promotes HKFs' migration and invasion depending on PTEN

After treatment with HMDE, NMDE or PBS, PTEN expression of HKFs was detected using qRT-PCR. The results demonstrated that HMDE significantly downregulated the

protein level of PTEN in HKFs (Figure 5a). To further confirm that downregulated PTEN increased the proliferation and motility of HKFs, we transfected HKFs with si-PTEN and the negative control. We also infected HKFs with adenoviral vector PTEN-GFP or adenoviral vector GFP, thus constructing

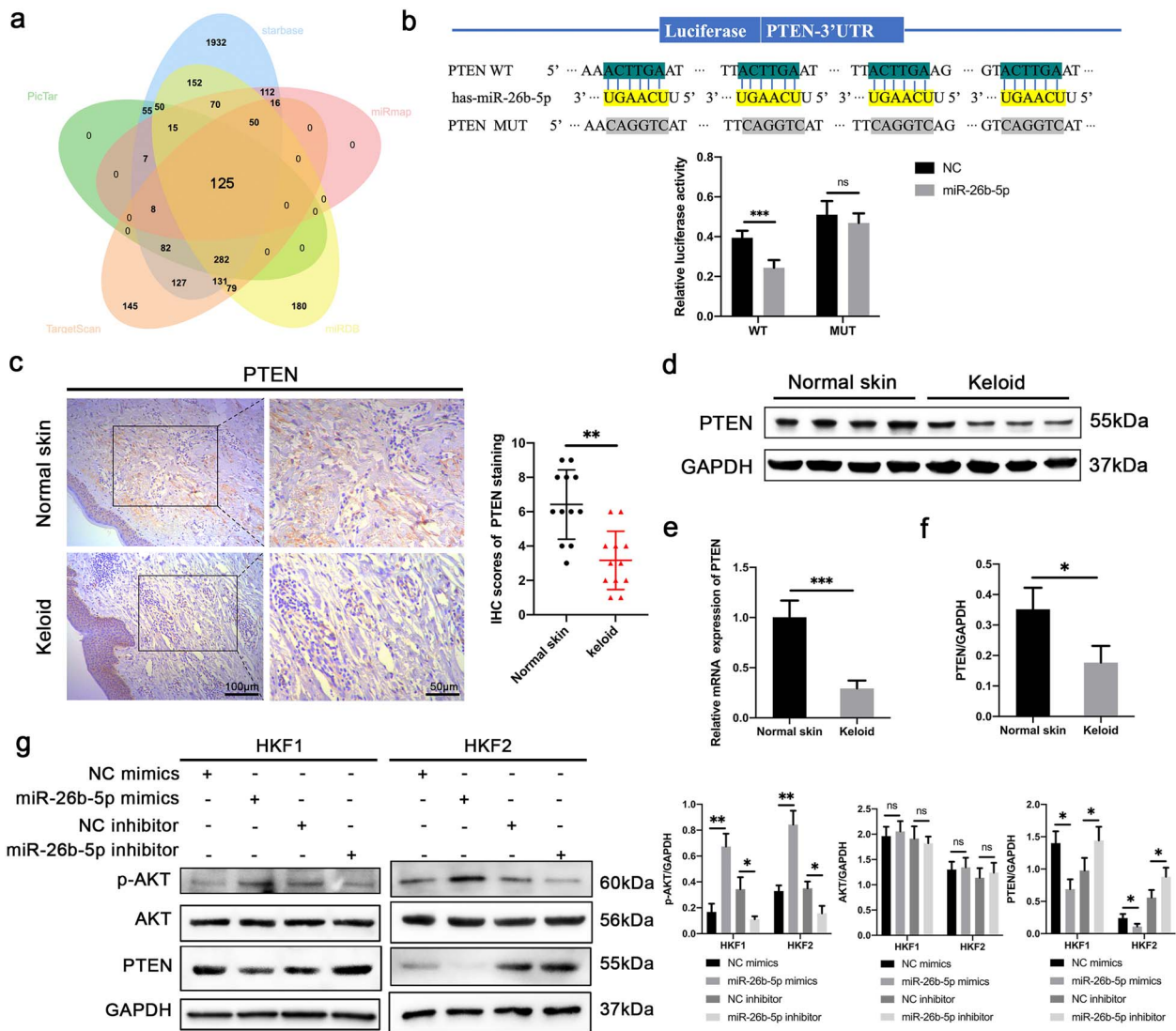


Figure 4. Exosmic miR-26b-5p inactivate PI3K/AKT pathway through PTEN targeting. (a) miRMap, PicTar, TargetScan, Starbase and miRDB predict the target genes of miR-26b-5p. (b) After co-transfecting wild-type or mutant PTEN 3'-UTR-driven luciferase vectors with miR-26b-5p mimics into HKFs, the luciferase activity was measured. The expression of PTEN was tested using IHC analysis (c), western blot (d) and qRT-PCR (e). (f) The relative expression of PTEN. (g) HKFs were transfected with miR-26b-5p mimics, miR-26b-5p inhibitor and their negative control. Western blot analysis measures the p-AKT, AKT and PTEN expression. * $p < 0.05$, ** $p < 0.01$, *** $p < 0.001$. WT wild-type, MUT mutant, UTR untranslated region, NC negative control, PTEN phosphatase and tension homolog

a PTEN-overexpressing stable cell line (LV PTEN-HKF1) and its corresponding negative control (LV NC-HKF1). The transfection efficiency was verified by western blot. As evident in Figure 5b, the overexpression of PTEN decreased p-AKT in HKFs whereas the inhibition of PTEN increased p-AKT in HKFs. The effectiveness of the adenoviral vector's transfection was evaluated using a fluorescence microscope (Figure S3a).

The CCK-8 assay confirmed that downregulation of PTEN expression enhanced the proliferation ability of HKFs (Figures 5c and S3b). The scratch and Transwell assays confirmed that downregulation of PTEN expression promoted the migration and invasion of HKFs (Figures 5e-f and S3c-d). Conversely, the overexpression of PTEN reduced the proliferation of HKFs (Figure 5d). The scratch and Transwell

assays confirmed that overexpression of PTEN reduced the migration and invasion of HKFs (Figures 5g-h).

Figure 5i reveals that the downregulation of PTEN in HKFs promotes the expression of MMP9 and α -SMA and inhibits the expression of E-cadherin. Conversely, upregulation of PTEN expression decreases MMP9 and α -SMA expression and increases E-cadherin expression. These data indicate that HMDE may promote fibrosis and EMT in HKFs by inhibiting PTEN expression.

Furthermore, to verify the co-action of miR-26b-5p and PTEN in HKFs, we co-transfected HKFs with NC mimics/miR-26b-5p mimics (50 nM) and LV NC/LV PTEN. The scratch and Transwell assays demonstrated that, following transfection of miR-26b-5p mimics, the LV PTEN could affect the migration and invasion of HKFs

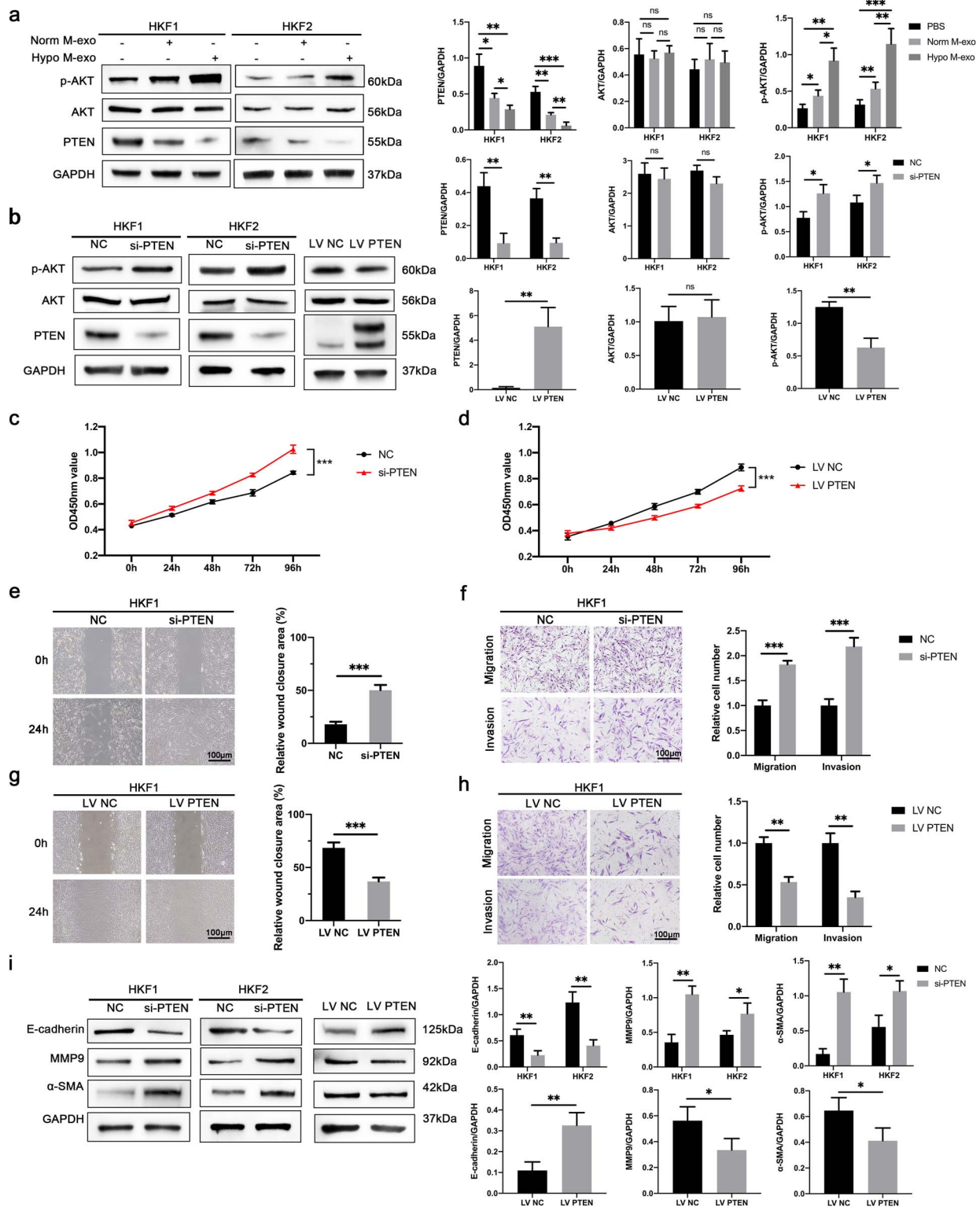


Figure 5. HMDE promoting HKFs' migration and invasion depends on PTEN. HKFs were treated with PBS, exosomes derived from normoxic or hypoxic macrophages. (a) Western blot analysis measures the p-AKT, AKT and PTEN expression in HKFs. (b) HKF1 were transfected with si-PTEN and the negative control or infected with adenoviral vector PTEN-GFP and adenoviral vector GFP. Western blot analysis measures the p-AKT, AKT and PTEN expression in HKFs. (c, d) CCK-8 assay represents the cell proliferation ability when PTEN is downregulated or overexpressed. Knockdown of PTEN in HKF1 by siRNA treatment. (e) Wound-healing assay. Scale bar, 100 μ m. (f) Cell migration and invasion assays utilizing Transwell or Matrigel-coated Transwell. Scale bar, 100 μ m. Overexpression of PTEN in HKF1 by adenoviral vector PTEN-GFP. (g) Wound-healing assay. Scale bar:100 μ m. (h) Cell migration and invasion assays utilizing Transwell or Matrigel-coated Transwell. Scale bar: 100 μ m. (i) Western blot analysis represents E-cadherin, MMP9 and α -SMA expression. ns not significant, * $p < 0.05$, ** $p < 0.01$, *** $p < 0.001$. si-PTEN small interfering RNA-PTEN, LV PTEN lentivirus-negative PTEN, LV NC lentivirus-negative control, Norm M-exo normoxic macrophage derived exosomes, Hypo M-exo hypoxic macrophage derived exosomes, HKF human keloid fibroblast, α -SMA α -smooth muscle actin, MMP9 matrix metalloprotein 9, E-cadherin epithelial cadherin

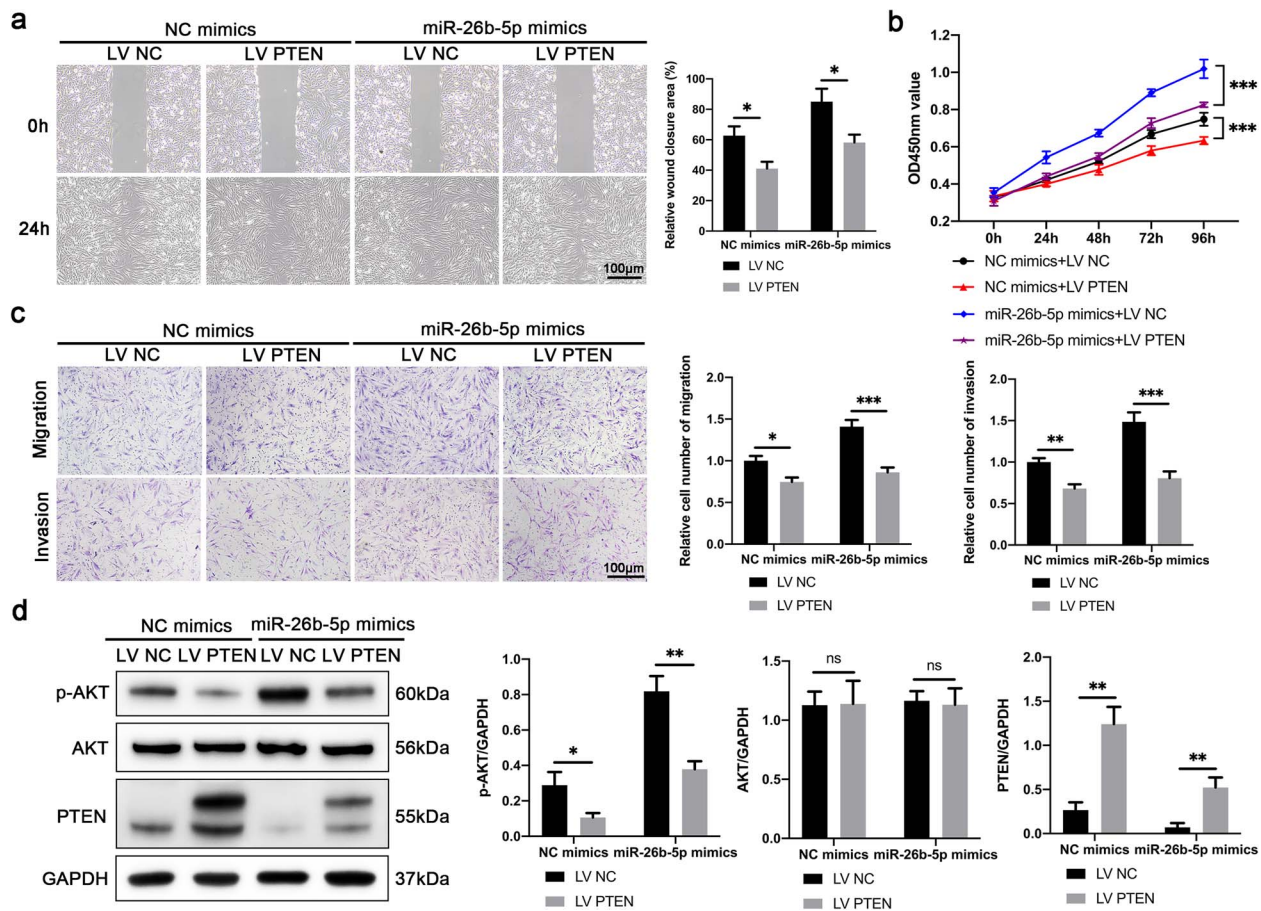


Figure 6. The co-action of miR-26b-5p and PTEN in HKFs. NC mimics/miR-26b-5p mimics and LV NC/LV PTEN were co-transfected into HKF1. (a) Wound-healing assay. Scale bar: 100 μ m. (b) CCK-8 assay represents the cell proliferation ability. (c) Cell migration and invasion assays using Transwell or Matrigel-coated Transwell. Scale bar: 100 μ m. (d) Western blot analysis represents p-AKT, AKT and PTEN expression. *ns* not significant, **p* < 0.05, ***p* < 0.01, ****p* < 0.001. *HKF* human keloid fibroblast, *LV PTEN* lentivirus-PTEN, *LV NC* lentivirus-negative control, *PTEN* phosphatase and tension homolog

(Figure 6a and c). The CCK-8 assay also confirmed that LV PTEN could affect HKFs' proliferation after transfecting miR-26b-5p mimics (Figure 6b). Western blot analyses demonstrated that overexpressing PTEN in HKFs could reverse the downregulation of PTEN and the upregulation of p-AKT caused by miR-26b-5p mimics (Figure 6d).

Discussion

Keloids are fibroproliferative skin diseases with malignant properties of persistent and aggressive growth [30]. Given that the hypoxic milieu is an important feature of keloids, it is imperative to comprehend the signal regulation and multiple interactions between macrophages and keloid fibroblasts under a hypoxic microenvironment.

We first explored the effect of hypoxic macrophages on the phenotype of HKFs. The CCK-8, cell scratch and Transwell assays confirmed that hypoxic macrophage supernatants could promote the proliferation, migration and invasion of HKFs. We extracted exosomes through ultracentrifugation to further clarify the specific components that play a role in the hypoxic macrophage supernatants. We identified the

collected exosomes through TEM, NTA and western blot analysis. We discovered that hypoxia enhances exosomes secretion in macrophages but does not affect the size or shape of exosomes, which is consistent with previous studies [31,32].

Exosome tracking technology verified that HKFs could take up both NMDE and HMDE. Hypoxia can increase the absorption of exosomes by HKFs, suggesting that macrophages may affect the phenotype of HKFs by exosomes. We found that HMDE can promote the proliferation, migration and invasion of HKFs. Combining our results, we demonstrated that CM collected from hypoxic macrophages promotes HKFs' proliferation, migration and invasion with the help of exosomes.

Based on these findings, we further studied the miRNAs carried by NMDE and HMDE. Recent research has demonstrated the important roles that exosomal miRNAs play in diseases such as inflammation [33,34], fibrosis [35–37] and cancer [38–40]. However, it is still unknown how macrophage exosomal miRNAs contribute to the pathogenesis of keloids. Exosomal-miRNA microarray analysis was used to examine the miRNA profiles of NMDE and HMDE,

and 38 DE miRNAs (18 upregulated and 20 downregulated) were identified. miR-26b-5p was one of the miRNAs that differed in expression between NMDE and HMDE and was upregulated in HMDE. Few current studies focus on the function of miR-26b-5p. In ischemic vascular disease, miR-26b can enhance endothelial cell survival, proliferation and angiogenesis [41]. miR-26b-5p exhibits oncogenic activity in glioma [42], lung cancer [43] and T-lymphocytic leukemia [44]. However, miR-26b-5p is downregulated in tumors such as hepatocellular carcinoma [45], breast cancer [46] and nasopharyngeal carcinoma [47], and plays a part in inhibiting the growth of tumors and inducing apoptosis. We validated miRNA expression in normal skin, keloid tissue, NMDE, HMDE and HKFs treated with NMDE or HMDE through qRT-PCR. The results showed that miR-26b-5p was highly expressed in HMDE and that HMDE shuttled miR-26b-5p into HKFs.

As a source of myofibroblasts, fibroblasts undergo the EMT process and are a major contributor to wound fibrosis [48]. EMT has been reported in keloids, manifested by a loss of epithelial cell markers such as E-cadherin and an increase in mesenchymal features such as α -SMA and vimentin, as well as enhanced cell motility and migration [49]. However, the underlying mechanisms of the EMT process in keloids are still not fully understood yet. In the current study, we demonstrated that HMDE can promote ECM synthesis, fibrosis and EMT in HKFs.

Further cellular function experiments were performed to investigate the potential role of miR-26b-5p in keloid formation. The findings revealed that the upregulation of miR-26b-5p significantly affected the proliferation, migration and invasion of HKFs *in vitro*, suggesting that miR-26b-5p may have potential as a biomarker for keloids. The genes targeted by miR-26b-5p were screened through bioinformatic databases including TargetScan, miRanda, starBase v.2.0 and PITA. The results demonstrated that PTEN was a miR-26b-5p downstream predicted by multiple databases. Specifically, exosomal miR-26b-5p derived from hypoxic macrophages can target PTEN directly. As one of the tumor suppressor genes, the mutation and deletion of PTEN are frequently observed in malignant tumors and fibrotic diseases [50–52]. Studies have demonstrated that a decreased expression of PTEN is observed in keloids [52]. In our studies, miR-26b-5p-mediated PTEN decrease resulted in increased PI3K/AKT signal activation, indicating that AKT may be engaged in miR-26b-5p/PTEN pathway. In addition, hypoxic macrophage-derived exosomal miR-26b-5p may affect targets other than PTEN in HKFs. Future research is required into these aspects.

This study investigated how HMDE affect keloid fibroblasts and how HMDE downregulates PTEN through miR-26b-5p to promote HKFs' proliferation, migration and invasion in keloids. We demonstrated that exosomes could transfer miR-26b-5p from macrophages to HKFs; this may probably enable HKFs to proliferate, migrate and invade more aggressively, allowing keloids to exhibit aggressive properties. However, exosomes derived from HKFs

to macrophages were not examined in this study. Here, we demonstrated that hypoxic macrophages could facilitate the metastasis of HKFs, although the impact of HKFs on macrophages was not investigated.

Collectively, our observations imply that the transfer of exosomes from hypoxic macrophages to HKFs explains how immune cells are involved in keloid progression, providing a potential therapeutic target for the future development of keloid treatment methods.

Conclusions

In conclusion, our study confirmed that the hypoxic environment of keloids promotes macrophage polarization to the M2 type and the release of macrophage-derived exosomes. miR-26b-5p primes the motility and proliferation of HKFs by inhibiting PTEN expression and activating the AKT- and EMT-related pathways.

Supplementary material

Supplementary material is available at *Burns & Trauma Journal* online.

Funding

This work was supported by the National Natural Science Foundation of China (81873937).

Data availability

All data needed to evaluate the conclusions in the paper are present in the paper and/or the Supplementary Materials. Additional data related to this paper may be requested from the authors. miRNA Sequencing data have been uploaded to <https://www.ncbi.nlm.nih.gov/sra/PRJNA891764>.

Ethics approval and consent to participate

The study was conducted in accordance with the Declaration of Helsinki, and approved by the Ethics Committee of the First Affiliated Hospital of Zhejiang University (no. 2014058; February 27, 2014).

Consent for publication

Informed consent was obtained from all subjects involved in the study.

Conflicts of interest

The authors declare that they have no conflict of interest.

References

1. Wu J, Del Duca E, Espino M, Gontzes A, Cueto I, Zhang N, *et al.* RNA sequencing keloid transcriptome associates keloids

- with Th2, Th1, Th17/Th22, and JAK3-skewing. *Front Immunol.* 2020;11:597741.
2. Andrews JP, Marttala J, Macarak E, Rosenbloom J, Uitto J. Keloids: the paradigm of skin fibrosis - Pathomechanisms and treatment. *Matrix Biol.* 2016;51:37–46.
 3. Limandjaja GC, Niessen FB, Scheper RJ, Gibbs S. The keloid disorder: heterogeneity, histopathology, mechanisms and models. *Front Cell Dev Biol.* 2020;8:360.
 4. Lee HJ, Jang YJ. Recent understandings of biology, prophylaxis and treatment strategies for hypertrophic scars and keloids. *Int J Mol Sci.* 2018;19:711.
 5. Braga T, Agudelo J, Camara N. Macrophages during the fibrotic process: M2 as friend and foe. *Front Immunol.* 2015;6:602.
 6. Shook B, Xiao E, Kumamoto Y, Iwasaki A, Horsley V. CD301b⁺ macrophages are essential for effective skin wound healing. *J Invest Dermatol.* 2016;136:1885–91.
 7. Kim H, Wang SY, Kwak G, Yang Y, Kwon IC, Kim SH. Exosome-guided phenotypic switch of M1 to M2 macrophages for cutaneous wound healing. *Adv Sci.* 2019;6:1900513.
 8. Krzyszczyk P, Schloss R, Palmer A, Berthiaume F. The role of macrophages in acute and chronic wound healing and interventions to promote pro-wound healing phenotypes. *Front Physiol.* 2018;9:419.
 9. Zhu Z, Ding J, Ma Z, Iwashina T, Tredget E. Alternatively activated macrophages derived from THP-1 cells promote the fibrogenic activities of human dermal fibroblasts. *Wound Repair Regen.* 2017;25:377–88.
 10. Wang Z, Zhao W, Cao Y, Liu Y, Sun Q, Shi P, et al. The roles of inflammation in keloid and hypertrophic scars. *Front Immunol.* 2020;11:603187.
 11. Jin Q, Gui L, Niu F, Yu B, Lauda N, Liu J, et al. Macrophages in keloid are potent at promoting the differentiation and function of regulatory T cells. *Exp Cell Res.* 2018;362:472–6.
 12. Xu X, Gu S, Huang X, Ren J, Gu Y, Wei C, et al. The role of macrophages in the formation of hypertrophic scars and keloids. *Burns Trauma.* 2020;8:tkaa006.
 13. Cramer T, Yamanishi Y, Clausen B, Förster I, Pawlinski R, Mackman N, et al. HIF-1 α is essential for myeloid cell-mediated inflammation. *Cell.* 2003;112:645–57.
 14. Zhang Z, Nie F, Kang C, Chen B, Qin Z, Ma J, et al. Increased periostin expression affects the proliferation, collagen synthesis, migration and invasion of keloid fibroblasts under hypoxic conditions. *Int J Mol Med.* 2014;34:253–61.
 15. Wang Q, Wang P, Qin Z, Yang X, Pan B, Nie F, et al. Altered glucose metabolism and cell function in keloid fibroblasts under hypoxia. *Redox Biol.* 2021;38:101815.
 16. Ma X, Chen J, Xu B, Long X, Qin H, Zhao RC, et al. Keloid-derived keratinocytes acquire a fibroblast-like appearance and an enhanced invasive capacity in a hypoxic microenvironment in vitro. *Int J Mol Med.* 2015;35:1246–56.
 17. Lei R, Li J, Liu F, Li W, Zhang S, Wang Y, et al. HIF-1 α promotes the keloid development through the activation of TGF- β /Smad and TLR4/MyD88/NF- κ B pathways. *Cell Cycle.* 2019;18:3239–50.
 18. Zhang Q, Wu Y, Ann DK, Messadi DV, Tuan T-L, Kelly AP, et al. Mechanisms of hypoxic regulation of plasminogen activator inhibitor-1 gene expression in keloid fibroblasts. *J Invest Dermatol.* 2003;121:1005–12.
 19. Ueda K, Yasuda Y, Furuya E, Oba S. Inadequate blood supply persists in keloids. *Scand J Plast Reconstr.* 2004;38:267–71.
 20. Wang G, Semenza G. General involvement of hypoxia-inducible factor 1 in transcriptional response to hypoxia. *Proc Natl Acad Sci USA.* 1993;90:4304–8.
 21. Song KX, Liu S, Zhang MZ, Liang WZ, Liu H, Dong XH, et al. Hyperbaric oxygen therapy improves the effect of keloid surgery and radiotherapy by reducing the recurrence rate. *J Zhejiang Univ-Sc B.* 2018;19:853–62.
 22. Vanni I, Alama A, Grossi F, Dal Bello MG, Coco S. Exosomes: a new horizon in lung cancer. *Drug Discov Today.* 2017;22:927–36.
 23. Zhu J, Liu B, Wang Z, Wang D, Ni H, Zhang L, et al. Exosomes from nicotine-stimulated macrophages accelerate atherosclerosis through miR-21-3p/PTEN-mediated VSMC migration and proliferation. *Theranostics.* 2019;9:6901–19.
 24. Ying W, Riopel M, Bandyopadhyay G, Dong Y, Birmingham A, Seo JB, et al. Adipose tissue macrophage-derived Exosomal miRNAs can modulate in vivo and in vitro insulin sensitivity. *Cell.* 2017;171:372–384.e12.
 25. Xun J, Du L, Gao R, Shen L, Wang D, Kang L, et al. Cancer-derived exosomal miR-138-5p modulates polarization of tumor-associated macrophages through inhibition of KDM6B. *Theranostics.* 2021;11:6847–59.
 26. Zhang J, Xu D, Li N, Li Y, He Y, Hu X, et al. Down-regulation of microRNA-31 inhibits proliferation and induces apoptosis by targeting HIF1AN in human keloid. *Oncotarget.* 2017;8:74623–34.
 27. Yan L, Wang L, Xiao R, Cao R, Pan B, Lv X, et al. Inhibition of microRNA-21-5p reduces keloid fibroblast autophagy and migration by targeting PTEN after electron beam irradiation. *Lab Investig.* 2020;100:387–99.
 28. Liu Y, Ren L, Liu W, Xiao Z. MiR-21 regulates the apoptosis of keloid fibroblasts by caspase-8 and the mitochondria-mediated apoptotic signaling pathway via targeting FasL. *Biochem Cell Biol.* 2018;96:548–55.
 29. Wang R, Bai Z, Wen X, Du H, Zhou L, Tang Z, et al. MiR-152-3p regulates cell proliferation, invasion and extracellular matrix expression through by targeting FOXF1 in keloid fibroblasts. *Life Sci.* 2019;234:116779.
 30. Lv W, Ren Y, Hou K, Hu W, Yi Y, Xiong M, et al. Epigenetic modification mechanisms involved in keloid: current status and prospect. *Clin Epigenetics.* 2020;12:183.
 31. King H, Michael M, Gleadle J. Hypoxic enhancement of exosome release by breast cancer cells. *BMC Cancer.* 2012;12:421.
 32. Jiang H, Zhao H, Zhang M, He Y, Li X, Xu Y, et al. Hypoxia induced changes of exosome cargo and subsequent biological effects. *Front Immunol.* 2022;13:824188.
 33. Yu H, Qin L, Peng Y, Bai W, Wang Z. Exosomes derived from hypertrophic Cardiomyocytes induce inflammation in macrophages via miR-155 mediated MAPK pathway. *Front Immunol.* 2021;11:606045.
 34. Lin YW, Nhieu J, Wei CW, Lin YL, Kagechika H, Wei LN. Regulation of exosome secretion by cellular retinoic acid binding protein 1 contributes to systemic anti-inflammation. *Cell Commun Signal.* 2021;19:69.
 35. Zhu HY, Li C, Bai WD, Su LL, Liu JQ, Li Y, et al. MicroRNA-21 regulates hTERT via PTEN in hypertrophic scar fibroblasts. *PLoS ONE.* 2014;9:e97114.
 36. Kashiyama K, Mitsutake N, Matsuse M, Ogi T, Saenko VA, Ujifuku K, et al. miR-196a downregulation increases the expression of type I and III collagens in keloid fibroblasts. *J Invest Dermatol.* 2012;132:1597–604.

37. Guo F, Carter DE, Leask A. miR-218 regulates focal adhesion kinase-dependent TGF β signaling in fibroblasts. *Mol Biol Cell*. 2014;25:1151–8.
38. Zhu X, Shen H, Yin X, Yang M, Wei H, Chen Q, *et al*. Macrophages derived exosomes deliver miR-223 to epithelial ovarian cancer cells to elicit a chemoresistant phenotype. *J Exp Clin Cancer Res*. 2019;38:81.
39. Nie Y, Chen J, Huang D, Yao Y, Chen J, Ding L, *et al*. Tumor-associated macrophages promote malignant progression of breast Phyllodes tumors by inducing myofibroblast differentiation. *Cancer Res*. 2017;77:3605–18.
40. Cooks T, Pateras I, Jenkins L, Patel K, Robles A, Morris J, *et al*. Mutant p53 cancers reprogram macrophages to tumor supporting macrophages via exosomal miR-1246. *Nat Commun*. 2018;9:771.
41. Martello A, Mellis D, Meloni M, Howarth A, Ebner D, Caporali A, *et al*. Phenotypic miRNA screen identifies miR-26b to promote the growth and survival of endothelial cells. *Mol Ther-Nucl Acids*. 2018;13:29–43.
42. Huse JT, Brennan C, Hambardzumyan D, Wee B, Pena J, Rouhanifard SH, *et al*. The PTEN-regulating microRNA miR-26a is amplified in high-grade glioma and facilitates gliomagenesis in vivo. *Genes Dev*. 2009;23:1327–37.
43. Liu B, Wu X, Liu B, Wang C, Liu Y, Zhou Q, *et al*. MiR-26a enhances metastasis potential of lung cancer cells via AKT pathway by targeting PTEN. *BBA*. 2012;1822:1692–704.
44. Mavrakis KJ, Van Der Meulen J, Wolfe AL, Liu X, Mets E, Taghon T, *et al*. A cooperative microRNA-tumor suppressor gene network in acute T-cell lymphoblastic leukemia (T-ALL). *Nat Genet*. 2011;43:673–8.
45. Ji J, Shi J, Budhu A, Yu Z, Forgues M, Roessler S, *et al*. MicroRNA expression, survival, and response to interferon in liver cancer. *New Engl J Med*. 2009;361:1437–47.
46. Zhang B, Liu XX, He JR, Zhou CX, Guo M, He M, *et al*. Pathologically decreased miR-26a antagonizes apoptosis and facilitates carcinogenesis by targeting MTDH and EZH2 in breast cancer. *Carcinogenesis*. 2011;32:2–9.
47. Lu J, He ML, Wang L, Chen Y, Liu X, Dong Q, *et al*. MiR-26a inhibits cell growth and tumorigenesis of nasopharyngeal carcinoma through repression of EZH2. *Cancer Res*. 2011;71:225–33.
48. Stone RC, Pastar I, Ojeh N, Chen V, Liu S, Garzon KI, *et al*. Epithelial-mesenchymal transition in tissue repair and fibrosis. *Cell Tissue Res*. 2016;365:495–506.
49. Yan L, Cao R, Wang L, Liu Y, Pan B, Yin Y, *et al*. Epithelial-mesenchymal transition in keloid tissues and TGF- β 1-induced hair follicle outer root sheath keratinocytes. *Wound Repair Regen*. 2015;23:601–10.
50. Tian Y, Li H, Qiu T, Dai J, Zhang Y, Chen J, *et al*. Loss of PTEN induces lung fibrosis via alveolar epithelial cell senescence depending on NF- κ B activation. *Aging Cell*. 2019;18:e12858.
51. Sang PF, Wang H, Wang M, Hu C, Zhang JS, Li XJ, *et al*. NEDD4-1 and PTEN expression in keloid scarring. *Genet Mol Res*. 2015;14:13467–75.
52. Kia V, Paryan M, Mortazavi Y, Biglari A, Mohammadi-Yeganeh S. Evaluation of exosomal miR-9 and miR-155 targeting PTEN and DUSP14 in highly metastatic breast cancer and their effect on low metastatic cells. *J Cell Biochem*. 2019;120:5666–76.